

Obstructed atomic insulators and superfluids of fermions coupled to \mathbb{Z}_2 gauge fields

Bhandaru Phani Parasar* and Vijay B. Shenoy†

Centre for Condensed Matter Theory, Department of Physics, Indian Institute of Science, Bangalore 560012, India

(Received 21 February 2023; accepted 16 June 2023; published 28 June 2023)

Studying spin- $\frac{1}{2}$ fermions coupled to \mathbb{Z}_2 gauge fields on the square lattice, we show how a spatial modulation of the fermion hopping amplitude allows for the realization of various obstructed atomic insulators that host higher-order band topology. Including the effect of quantum dynamics of the gauge fields within a simplified model, we find a rich phase diagram of this system with a number of superfluid phases (which host distinct types of topological defects) arising from the attractive interactions mediated by the gauge fields. The evolution of the superfluid obtained by the destabilization of the obstructed atomic insulators from the Bardeen-Cooper-Schrieffer (BCS) type to a Bose-Einstein condensate (BEC) of tightly bound pairs occurs via the realization of these different superfluid phases separated by first-order transitions.

DOI: [10.1103/PhysRevB.107.245142](https://doi.org/10.1103/PhysRevB.107.245142)**I. INTRODUCTION**

The discovery of strong topological phases of noninteracting fermions [1–10] marks an important milestone, even offering new technological advances [11,12]. Recent theoretical work has revealed that a more general characterization of topology can be realized in terms of obstructed atomic limits [13–17], leading to the notion of higher-order topological insulating (HOTI) phases [18]. HOTIs have been realized in a number of systems [19–23].

An important concurrent direction is the investigation of the consequences of these ideas in the presence of strong interactions and correlations. Many approaches to strongly correlated systems/frustrated magnetism [24–34] lead to problems of matter coupled to dynamical gauge fields [35], and are encouraged by the possibilities of their realization in experiments [36–38].

Recent studies of gauge fields coupled to charged fermions have led to the identification of novel phases and phase transitions, e.g., the orthogonal metallic phase in an exactly solvable model [39]. Using a numerical quantum Monte Carlo (QMC) formulation for \mathbb{Z}_2 lattice gauge coupled fermions, Ref. [40] showed that π flux phase [41] with emergent Dirac fermions is spontaneously generated upon the increase of the fermion hopping amplitude. Tuning the quantum dynamics of the gauge fields, a continuous transition from the deconfined Dirac phase to confined BEC with the simultaneous onset of confinement of the gauge fields and symmetry breaking is found. Studies on closely related models [42–46] show several exotic phases and phase transitions.

The developments noted above motivate broader questions. Can systems with matter coupled to gauge fields be designed to realize interesting fermionic phases with different patterns of short-range entanglement? For example, can they produce

obstructed atomic insulators (OAI) discussed above? What is the fate of such phases when the dynamics of the gauge fields are included? We address these questions in the paper.

The model we study in this paper has spatially varying hoppings of spin- $\frac{1}{2}$ fermions coupled to the gauge fields. Using a pattern of hoppings shown in Fig. 1, we obtain a variety of phases, in the absence of quantum dynamics of the gauge fields, including a metal, Dirac semimetal, trivial band insulators, and OAI when the strengths of the fermion hopping and the modulation of the hopping pattern are tuned. Several variants of OAI are realized in the *same system*. We explore the effects of quantum dynamics of the gauge fields in a simplified model following Ref. [44], which captures the deconfined phase of the gauge fields and results in a local attractive interaction between the fermions. We show that turning on the interaction induced by the gauge fields destabilizes these phases resulting in a rich phase diagram that includes a variety of superfluid/density-ordered phases, magnetically ordered phases, and valence bond solid phases with gapped (massive) fermions. An interesting finding is that the crossover from the BCS-type superfluid phases (for attractive interactions) obtained from the nontrivial phases cross over to the BEC phase of tightly bound pairs, through a set of distinct superfluid phases, which are separated by first-order transitions in stark contrast to an insulator with a local attractive interaction which has a smooth crossover [47,48]. We also study the nature of the phase transitions between these phases using field theoretic techniques uncovering the difference between topologically trivial mass and that which produces an OAI phase.

II. MODEL

We work on a square lattice with a four-site basis consisting of sites A_1, A_2, B_1, B_2 as shown in Fig. 1. At each site of the lattice, fermions are created by the operator $c_{Ia\sigma}^\dagger$ where I is the unit cell index, $a \in \{A_1, A_2, B_1, B_2\}$, and σ is a two-component spin (flavor) index. Along each link of

*bhandarup@iisc.ac.in

†shenoy@iisc.ac.in

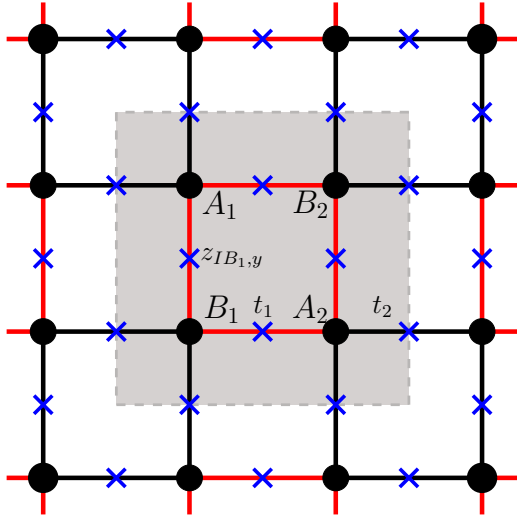


FIG. 1. Fermions coupled to gauge fields on a square lattice; unit cell is shaded. The hoppings are spatially varying with the pattern shown: red links are $t_1 = t(1+r)$ and black links are $t_2 = t(1-r)$. Blue crosses show the gauge qubits.

this lattice, there is a gauge qubit whose Pauli-Z operator is denoted by $Z_{Ia,\alpha}$, where $\alpha \in \{x, y\}$ indicates the direction of the link emanating from the site Ia . The fermions couple to the gauge fields via their hopping amplitudes $t_{Ia,\alpha}$ and the system's Hamiltonian is

$$\begin{aligned} \mathcal{H}' = & - \sum_{Ia,\alpha,\sigma} (t_{Ia,\alpha} c_{(Ia+\alpha)\sigma}^\dagger (Z_{Ia\alpha})^{q_\sigma} c_{Ia\sigma} + \text{H.c.}) \\ & - \mu \sum_{Ia} n_{Ia} - K \sum_p B_p - K' \sum_{Ia,\alpha} X_{Ia,\alpha}, \end{aligned} \quad (1)$$

where $(Ia + \alpha)$ is the site reached by traveling along the α link emanating from Ia ; $t_{Ia,\alpha}$ is the hopping amplitude; q_σ is a \mathbb{Z}_2 valued charge (i.e., 0 or 1) of the fermion with spin $\sigma \in \{\uparrow, \downarrow\}$; μ is the chemical potential; $n_{Ia} = \sum_\sigma c_{Ia\sigma}^\dagger c_{Ia\sigma}$; p is a plaquette; $B_p = \prod_{(Ia,\alpha)/p} Z_{Ia,\alpha}$ is the plaquette magnetic term where the product is over all links that touch the plaquette p ; K is the inverse magnetic permeability; $X_{Ia,\alpha}$ is the Pauli X operator on the link (Ia, α) ; and K' is the dielectric constant. The key aspect of this model is the spatially varying hoppings where $t_{Ia,\alpha}$ takes on the value t_1 for links inside the unit cell (Fig. 1) and t_2 for links that cross from one unit cell to another. We parametrize $t_{1,2} = t(1 \pm r)$, where t is a scale of the kinetic energy and r a dimensionless parameter, and assume periodic boundary conditions.

The model in Eq. (1) has a global $U(1)$ phase symmetry that corresponds to the conservation of the total number of particles. If the \mathbb{Z}_2 charges of the fermions are independent of spin, i.e., $q_\sigma = q$, then the system has a global $SU(2)$ symmetry that acts on the spin labels, as assumed here. It has time reversal symmetry Θ , with $\Theta^2 = -1$. Further, there is a local ‘‘gauge symmetry,’’ in that the unitary operators $G_{Ia} = A_{Ia}(-1)^{q n_{Ia}}$ transform \mathcal{H}' back to itself, with $A_{Ia} = \prod_{(Ia,\alpha)/Ia} X_{Ia,\alpha}$, where the product is over all the links that start or terminate at Ia . The physical Hilbert space of the theory is that subspace where each G_{Ia} acts as an identity, i.e.,

the Gauss law condition $G_{Ia} = 1, \forall Ia$. Physically, this entails the absence of any external charges.

If the fermions are not \mathbb{Z}_2 charged (i.e., $q = 0$), the ground state is a direct product of the Fermi-sea determined by μ and that of the \mathbb{Z}_2 gauge theory. The \mathbb{Z}_2 gauge theory is in a deconfined phase [49] for $K'/K \lesssim 0.22$, and in a confined phase for larger values of K'/K . In the remainder of the paper, we focus on $q = 1$ and half-filling of fermions.

III. GROUND STATE PHASE DIAGRAM

A. $K' = 0$

Although $K' = 0$ suppresses the dynamics of the gauge fields, it reveals the physics that emerges from the competition between the kinetic energy of the fermions and the plaquette magnetic energy. Noting that $B_p, \forall p$ are conserved quantities when $K' = 0$, we can write down the ground state wave function of the system for a particular set of values of B_p . If $z_{Ia,\alpha} \in \pm 1$ (eigenvalue of $Z_{Ia,\alpha}$) describes the gauge fields that realize [50] the given B_p s, the ground state $|\psi_{GS}\{z_{Ia,\alpha}\}\rangle = (\prod_{Ia} \frac{(1+G_{Ia})}{\sqrt{2}}) [(\prod_{Ia\alpha} |z_{Ia,\alpha}\rangle) \otimes |\text{FS}\{z_{Ia,\alpha}\}\rangle]$, where $|\text{FS}\{z_{Ia,\alpha}\}\rangle$ is the Fermi sea, is attained by those B_p that minimize the energy.

To determine optimal B_p s, we search among those that are translationally invariant with the unit cell shown in Fig. 1. The ground state phase diagram (with eight distinct phases) is shown in Fig. 2. For small $|r| \lesssim 0.1$, we obtain a metal M_0 with zero flux per plaquette. There is a first-order transition at a critical t/K to a gapped phase AI_2 for $r > 0$ and OAI_2 for $r < 0$. In the AI_2 phase ($r > 0$), all the plaquettes in the unit cell except the one that is enclosed by links with the black t_2 hopping obtain a π flux, while the OAI_2 gapped phase has π flux in all plaquettes except that bounded by the red t_1 hoppings. At an even higher value of t/K , we see that gapped phases AI_1 ($r > 0$) and OAI_1 ($r < 0$) are obtained where a uniform π flux is realized. For larger values of $|r|$, $|r| \gtrsim 0.17$ an additional gapped phase (there is also an intervening metallic phase M_3 that appears), AI_3 ($r > 0$) and OAI_3 ($r < 0$), appears between the metal M_0 and the AI_2/OAI_2 phases. For $r = 0$, we find that the metal M_0 undergoes a transition to a gapped phase (AI_2 or OAI_2 depending on $r \rightarrow \pm 0$) at $t/K = 6.72$ and remains in this phase until $t/K = 6.92$, at which there is a first-order transition to a gapless Dirac semimetal with a uniform π flux. This is consistent with Ref. [40], which, however, did not report the intervening gapped phase separating the metal and the Dirac semimetal. We note that the Dirac semimetal at $r = 0$ has a diminished unit cell which encloses $\pi \pmod{2\pi}$ \mathbb{Z}_2 flux, whereas unitcell of OAI_1 or AI_1 ($r \neq 0$) has $0 \pmod{2\pi}$ \mathbb{Z}_2 flux. Thus, the Dirac semimetal and OAI_1 are distinct projective representations of the square lattice translation symmetry, and the band gap of OAI_1 must vanish as $r \rightarrow 0$. In contrast, the diminishing of the unit cell does not occur for OAI_2 when $r \rightarrow 0$, indicating that it can remain gapped.

Properties of gapped phases

Are the gapped phases similar or distinct? To address this, we first observe that all of the phases (Fig. 2) have a fourfold rotational symmetry C_4 . Next, we resolve the space

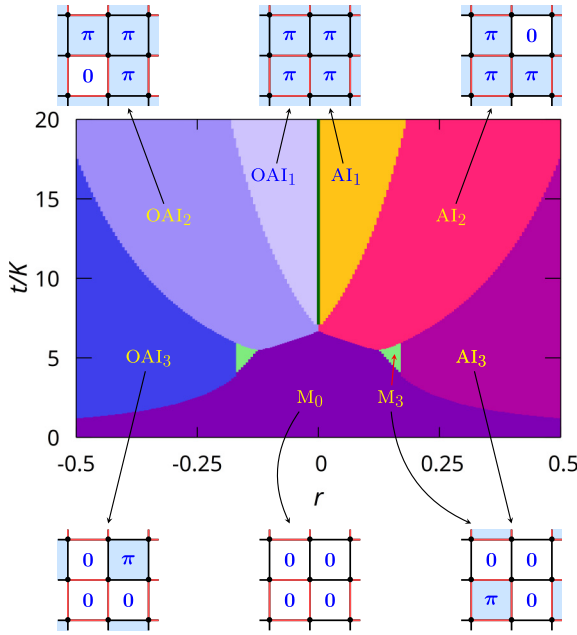


FIG. 2. Ground state phase diagram of Eq. (1) with $K' = 0$. Key: M—metals, AI—atomic insulators, OAI—obstructed atomic insulators. Flux patterns realized in each phase are indicated by the dark arrows.

of occupied fermionic states at high symmetry points $\Gamma = (0, 0)$, $M = (\pi, \pi)$, and $X = (\pi, 0)$ in the Brillouin zone of the larger unit cell into one-dimensional irreps of C_4 rotations (Table I and [51], Sec. S1). In the AI phases ($r > 0$), the representations realized at the Γ and M points are the same—such insulators have been termed as *atomic insulators* [52,53] and hence the title AI for these phases. On the other hand, remarkably, we see that the OAI insulators ($r < 0$) have different representations at the different high-symmetry points and are *obstructed atomic insulators* [52,53], hence titled OAI. OAIs are characterized by corner modes (with energies in the gap) in systems with open boundary conditions and have a filling anomaly [52], which we have verified. ([51], S2)

A further natural question pertains to the distinction between different OAI phases. Interestingly, we find that all these are the same phase in that they carry the same classification data. In fact, we have found a way to connect the single particle hamiltonians of OAI₂ and OAI₃ through an adiabatic path (breaking time-reversal symmetry and not invoking the gauge fields) that retains the gap throughout, demonstrating

TABLE I. Number of irreps of C_4 rotations labeled by $\lambda_p = e^{i\frac{2\pi}{n}p}$ at high symmetry points in the Brillouin zone. $n = 4$ for Γ and M , and $n = 2$ for X .

Phase	HSP	# λ_0	# λ_1	# λ_2	# λ_3
OAI _{1/2/3}	Γ	2	4	6	4
	M	4	4	4	4
	X	8	8	—	—
AI _{1/2/3}	Γ	4	4	4	4
	M	4	4	4	4
	X	8	8	—	—

that the phase OAI₂ and OAI₃ are topologically indistinct. Note, however, that the flux patterns are distinct in these two phases, yet both of them realize the same fermionic band topology.

B. $K' \neq 0$

Next, we investigate the fate of these phases when the dynamics of the gauge fields are turned on, i.e., $K' \neq 0$. In this case, the phase diagram has to be obtained with the recourse to quantum Monte Carlo simulations as in [40,43]. Here we adopt a simpler approach following Ref. [44], which suggested coupling the fermions to the toric code [54]. This entails replacing the dielectric term $-K' \sum_{Ia,\alpha} X_{Ia,\alpha}$ by $-h \sum_{Ia} A_{Ia}$. If this is achieved by a perturbation expansion of the \mathbb{Z}_2 gauge theory (in the absence of the fermions), then $h \sim (K')^4/K^3$, taking the gauge theory to the toric code limit, which is valid for $|K'/K| \ll 1$. This is the deconfined phase of the gauge theory. In this paper, we treat h as an independent parameter that can take any real value, i.e., we couple the fermions to a toric code. The key physical consequence of this formulation is that the gauge theory in the toric code limit is always in the deconfined phase. Although this approach cannot shed light on the confinement transition and its effect on the fermions, as shown below, it does display much interesting physics.

Within this simpler approach, the Gauss law constraint can be “solved” as $A_{Ia} = (-1)^{n_{Ia}} = 4(n_{Ia,\uparrow} - \frac{1}{2})(n_{Ia,\downarrow} - \frac{1}{2})$ leading to the hamiltonian

$$\begin{aligned} \mathcal{H} = & - \sum_{Ia,\alpha,\sigma} (t_{Ia,\alpha} c_{(Ia+\alpha)\sigma}^\dagger (Z_{Ia\alpha})^{q\sigma} c_{Ia\sigma} + \text{H.c.}) \\ & - \mu \sum_{I,a} n_{Ia} - K \sum_p B_p - 4h \sum_{Ia} \left(n_{Ia,\uparrow} - \frac{1}{2} \right) \\ & \times \left(n_{Ia,\downarrow} - \frac{1}{2} \right), \end{aligned} \quad (2)$$

which is the Hubbard model [55] coupled to gauge fields. As we will see below, the presence of this coupling to the gauge fields produces interesting physics not present in the usual Hubbard model. At half-filling, $\mu = 0$, and there is an enlarged global symmetry $SU_{\text{ph}}(2) \times SU_{\text{sp}}(2) \sim SO(4)$ which includes particle-hole (ph) transformations and spin (sp) rotations [56]. We use a version of the hamiltonian that makes this symmetry manifest, see [51] (Sec. S3),

I. $h > 0$

The physics of the resulting attractive Hubbard model is well captured by a mean-field analysis, taking care to note the mentioned $SU_{\text{ph}}(2) \times SU_{\text{sp}}(2)$ symmetry. For $h > 0$, the broken $SU_{\text{ph}}(2)$ symmetry is described by a three component order parameter ([51], Sec. S3) with magnitude Δ that allows a transformation between the superconducting (SC) and (π, π) density wave phase, referred to as “SCD superfluid.” When $h \ll t$, the metallic phase M_0 undergoes a BCS instability for any value of $h > 0$ to an SCD phase with large pairs $\Delta \ll 1/2$. For larger values of h , these pairs evolve into tightly bound bosons, and the superfluid for $h \gg t$ is a condensate of

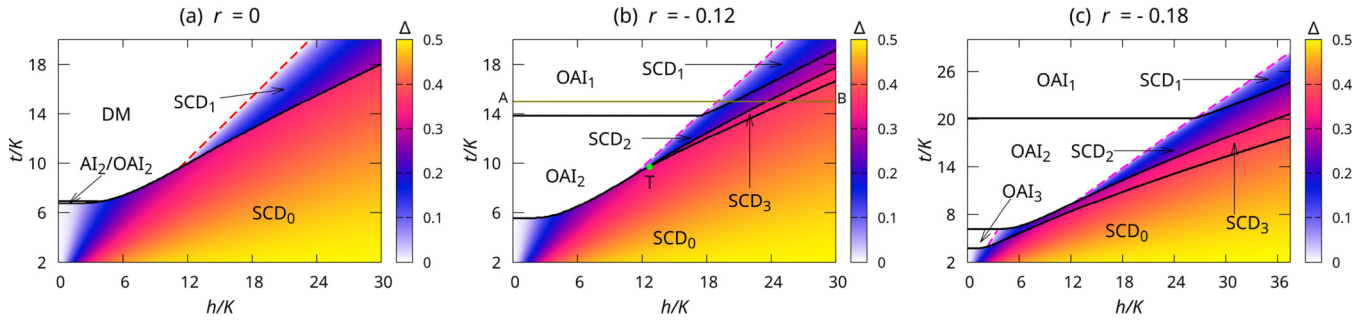


FIG. 3. Mean-field phase diagram of Eq. (2). The color shows the magnitude of the SCD order parameter Δ . Solid black lines indicate first-order transitions. The dashed red line in panel (a) is a continuous transition of the Gross-Neveu type. Dashed magenta lines in panels (b) and (c) denote a continuous transitions of $O(3)$ - ϕ^4 universality. In (b), the bullet point in light green marked T is the triple point with the coexistence of SCD_0 , SCD_2 , and SCD_3 . On the line marked A-B, the evolution of superfluid from the BCS state to the BEC occurs via a sequence of first order transitions.

such bosons ($\Delta \approx \frac{1}{2}$). This is obtained for $t/K \leq 6.72$, $r = 0$ as is shown in Fig. 3(a), where the superfluid phase is labeled SCD_0 to denote the parent M_0 unpaired phase. For $6.72 \leq t/K \leq 6.92$, the gapped OAI_2/AI_2 phase is stable for $h \ll t$, but undergoes a *first-order transition* to the SCD_0 superfluid for larger values of h . For $6.72 < t/K < 10.0$, the Dirac metal (DM) obtained at $h = 0$ is stable for finite h , and upon an increase of h , undergoes a first-order transition to the SCD_0 phase. For $t/K > 10.0$, the DM phase itself undergoes a *continuous transition* (more on this below) to an SCD phase denoted by SCD_1 to indicate the uniform π -flux background of the parent normalstate. Interestingly, for larger values of h , the SCD_1 yields to the lower energy SCD_0 phase (which is a BEC of fermionpairs for large h) via a first-order transition.

2. Instability of OAI phases

Matters put on an exciting hue when $r \neq 0$. For $r = -0.12$, as shown in Fig. 3(b), the insulator OAI_2 obtained at $t/K \gtrsim 5.5$ is stable to paring at small $h \ll t$, and upon the increase of h undergoes a phase transition to the SCD_0 phase via a first-order transition. However, for $10 \lesssim t/K \lesssim 14$, the OAI_2 undergoes a superfluid instability of its own and transits to an SCD_2 superfluid via a *continuous* transition [48]. Interestingly, for larger h , the SCD_2 phase transforms to an SCD_3 , a superfluid phase whose parent normal state is the OAI_3 phase! The SCD_3 phase, again, undergoes a first-order transition to an SCD_0 phase at even larger values of h . An interesting aspect of the phase diagram is the presence of an SCD triple point ($t/K = 9.7$, $h/K = 12.7$) where SCD_0 , SCD_2 , and SCD_3 phases coexist. For $t/K \gtrsim 14$ [see the horizontal line marked A-B in 3(b)], the OAI_1 phase, stable at small h , undergoes a continuous phase transition to the SCD_1 phase (whose parent normal state is the OAI_1 phase). The phase eventually evolves to the SCD_0 phase, via three first-order transitions, first from SCD_1 to SCD_2 , the second from SCD_2 to SCD_3 , and the third from SCD_3 to SCD_0 . There is an even richer phase diagram [Fig. 3(c)] obtained for $r = -0.18$, where three distinct OAIs are realized at $h = 0$. There are regimes of t/K where each of these insulators OAI_i ($i = 1, 2, 3$) undergoes a continuous transition to an SCD_i phase; all of these evolve to the SCD_0 (BEC of pairs) phase via a sequence of first-order transitions up on the increase of h . This is the key

new physics that emerges due to the coupling of the fermions to the gauge fields in that the crossover from the BCS state obtained by the destabilization of an OAI by the attractive interactions induced by the guage fields evolves to a BEC state via a sequence of intermediate superfluid states (SCD_i , $i > 0$), eventually attaining the SCD_0 which is what is realized in the Hubbard model (without coupling to gauge fields) [47,48].

3. Discussion of SCD phases

The dispersion of the Bogoliubov quasiparticles in the SCD phases indicate that they are all topologically trivial. They also have an identical long wave length description in terms of an $O(3)$ nonlinear- σ model (without any topological; even number of fermion flavors [57]). The difference between these phases will be found only in the cores of solitonic fields of the order parameter like skyrmions [57], which may host localized fermionic modes.

4. Phase Transitions

Turning to the nature of phase transitions between various phases, while many are first order, those between OAI_i and SCD_i ($i = 1, 2, 3$) are continuous. The critical theory is described by an $O(3)$ symmetric ϕ^4 theory in $2 + 1$ dimensions [58]. The most interesting continuous transition is the one between the DM to the SCD_1 phase. As detailed in [51] (Sec. S4), this is captured by $O(N_\Sigma)$ Gross-Neveu theory [59–61], where $N_\Sigma = 3$ here, with gapless Dirac fermions and an $O(N_\Sigma)$ symmetric four-fermion term with a coupling constant $g(\sim h)$. The physics of the masses that induce the OAI phase can be studied by including an additional mass term of the form $\mathbf{m} \cdot \mathbf{\Lambda} = \sum_b m_b \Lambda_b$ (where Λ_b is a set of matrices that anticommute with the Dirac gamma matrices). Performing a one-loop renormalization group analysis ([51], Sec. S5), we obtain the flow equations $s\partial_s g = -\epsilon g + \frac{4N_\Sigma + N_\gamma - 6}{\pi} g^2$, $s\partial_s m_b = m_b(1 + \frac{N_\Sigma}{\pi} g)$ with $D = 2 + \epsilon$, where $D = 3$ is the space-time dimension, $N_\gamma = 8$, and $s \rightarrow \infty$ is the infrared limit, with two fixed points. The first one at $(g = 0, m_b = 0)$ is the gapless Dirac theory, stable to small perturbations. The second one is the Gross-Neveu fixed point at $(g = \frac{\pi\epsilon}{4N_\Sigma + N_\gamma - 6}, m_b = 0)$ obtains the critical interaction strength that destabilizes the Dirac fermions. We compute the anomalous dimensions η of mass operators that produce OAI_1 phases to compare them

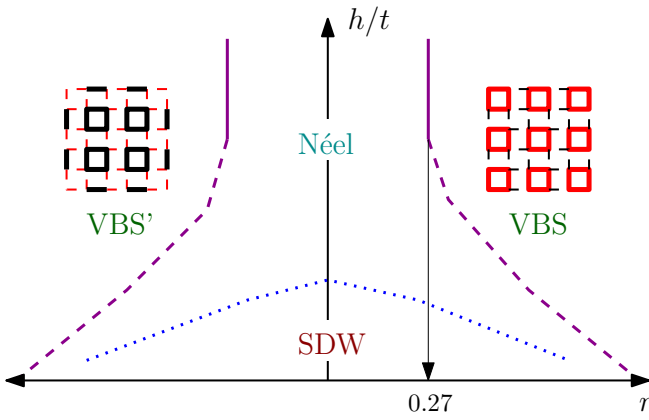


FIG. 4. Schematic phase diagram for $h < 0$ (repulsive case). The phase boundary between the Néel state and the VBS states obtained at a large value of $h/t \gg 1$ is obtained using a Schwinger boson mean-field theory where $r_c = 0.27$. The dashed lines are schematic phase boundaries. The dotted line between the SDW (spin density wave state) and Néel state represents a crossover. The region denoted by SDW can contain a rich structure with several phases like SDW_i ($i = 1, 2, 3$) depending on the value of t/K .

with mass that produces a trivial gapped phase to find that $\eta_{\text{OAI}_i} = \frac{\epsilon N_\Sigma}{4N_\Sigma + N_\nu - 6}$, $\eta_{\text{Trivial}} = -\frac{\epsilon N_\Sigma}{N_\nu - 2}$. The interesting point is that these two anomalous dimensions are of opposite sign.

We conclude the discussion of the $h > 0$ phase diagram by noting that one obtains very similar physics for $r > 0$, where one obtains a similar phase diagram involving SCD phases obtained by destabilizing AI_i ($i = 1, 2, 3$) to obtain SCD'_i phases.

5. Phase diagram for $h < 0$

We have also studied the $h < 0$ phase diagram using available methods [62–66] where valence bond and Néel ordered states are realized. The mean field phase diagram for $h < 0$, which results in the repulsive Hubbard model, can be obtained by studying the symmetry breaking in the spin sector (preserving the particle-hole symmetry), which again leads to an $\text{O}(3)$ vector order parameter (identifiable as the Néel order parameter). This again leads to spin-density wave SDW_i (SDW'_i) phases obtained by destabilizing OAI_i (AI_i) phases ($i = 1, 2, 3$). This mean-field analysis is, however, not re-

liable when $|h| \gg t$, where the system is a Mott insulator with forbidden double occupancy. The effective low-energy theory of the system becomes a Heisenberg model (irrespective of which insulator is the parent state) with $\mathcal{H}_H = -\sum_{Ia,I'a'} J_{Ia,I'a'} \mathbf{S}_{Ia} \cdot \mathbf{S}_{I'a'}$, where $J_{Ia,I'a'} \sim t_1^2/h$ on links inside the unit cell (Fig. 1) and $J_{Ia,I'a'} \sim t_2^2/h$ on links across unit cells. For $r \sim 1$, the ground state for small t/h is a valence bond solid (VBS) where the spins form resonating singlets on the links inside the unit cell. For $r \sim -1$, we obtain spins resonating on plaquettes bounded by dark-colored links in Fig. 1. The state for $r = 0$ is a Néel antiferromagnet (AF). We thus expect a transition from a Néel state to the valence bond state (cf. [62]) with the increase of $|r|$. The critical point $|r_c| = 0.27$ can be located using the Schwinger boson mean-field theory [63–65] as detailed in [51], Sec. 6. The full phase diagram (see Fig. 4) on the repulsive side involves several SDW_i phases, which are smoothly connected to the Néel phase, the details are left for future study.

IV. CONCLUDING REMARKS

This paper reveals the remarkable possibilities of realizing interesting phases in a system where fermions are coupled to gauge fields with spatially modulated hopping amplitudes. Our key results include the realization of various OAI in these systems along with their instabilities. The study of the quantum dynamics of the gauge fields leads to another interesting finding, i.e., the nature of the BCS to BEC cross-over in systems where fermions are coupled to gauge fields is much richer with many intervening phases. It will be interesting to explore realization of this model in cold atomic systems (cf., [38]). Exploration of these ideas in other problems, such as frustrated magnetism and lattice gauge theory, are also fruitful directions. For example, if the gauge theory described in Eq. (1) arose from a partonic construction of a strongly correlated problem, then the physical fermions would be the product of the c fermions and an Ising spin [39,67]. In this scenario, the interesting insulating phases such as OAI_i ($i = 1, 2, 3$) are more appropriately called *orthogonal* obstructed atomic insulators, OAI_i^* [39].

ACKNOWLEDGMENT

The authors acknowledge support from SERB, DST, India via the CRG scheme. B.P.P. acknowledges support received through the PMRF program.

[1] A. Kitaev, *AIP Conf. Proc.* **1134**, 22 (2009).
 [2] S. Ryu, A. P. Schnyder, A. Furusaki, and A. W. W. Ludwig, *New J. Phys.* **12**, 065010 (2010).
 [3] M. Z. Hasan and C. L. Kane, *Rev. Mod. Phys.* **82**, 3045 (2010).
 [4] X.-L. Qi and S.-C. Zhang, *Rev. Mod. Phys.* **83**, 1057 (2011).
 [5] C.-K. Chiu, J. C. Y. Teo, A. P. Schnyder, and S. Ryu, *Rev. Mod. Phys.* **88**, 035005 (2016).
 [6] C. L. Kane and E. J. Mele, *Phys. Rev. Lett.* **95**, 146802 (2005).
 [7] L. Fu, C. L. Kane, and E. J. Mele, *Phys. Rev. Lett.* **98**, 106803 (2007).
 [8] L. Fu and C. L. Kane, *Phys. Rev. B* **76**, 045302 (2007).

[9] J. E. Moore and L. Balents, *Phys. Rev. B* **75**, 121306(R) (2007).
 [10] R. Roy, *Phys. Rev. B* **79**, 195322 (2009).
 [11] J. L. Collins, A. Tadich, W. Wu, L. C. Gomes, J. N. B. Rodrigues, C. Liu, J. Hellerstedt, H. Ryu, S. Tang, S.-K. Mo, S. Adam, S. A. Yang, M. S. Fuhrer, and M. T. Edmonds, *Nature (London)* **564**, 390 (2018).
 [12] M. J. Gilbert, *Commun. Phys.* **4**, 70 (2021).
 [13] R.-J. Slager, A. Mesaros, V. Juričić, and J. Zaanen, *Nat. Phys.* **9**, 98 (2013).
 [14] W. A. Benalcazar, B. A. Bernevig, and T. L. Hughes, *Science* **357**, 61 (2017).

- [15] W. A. Benalcazar, B. A. Bernevig, and T. L. Hughes, *Phys. Rev. B* **96**, 245115 (2017).
- [16] Z. Song, Z. Fang, and C. Fang, *Phys. Rev. Lett.* **119**, 246402 (2017).
- [17] J. Langbehn, Y. Peng, L. Trifunovic, F. von Oppen, and P. W. Brouwer, *Phys. Rev. Lett.* **119**, 246401 (2017).
- [18] F. Schindler, A. M. Cook, M. G. Vergniory, Z. Wang, S. S. P. Parkin, B. A. Bernevig, and T. Neupert, *Sci. Adv.* **4**, eaat0346 (2018).
- [19] F. Schindler, Z. Wang, M. G. Vergniory, A. M. Cook, A. Murani, S. Sengupta, A. Y. Kasumov, R. Deblock, S. Jeon, I. Drozdov, H. Bouchiat, S. Guéron, A. Yazdani, B. A. Bernevig, and T. Neupert, *Nat. Phys.* **14**, 918 (2018).
- [20] M. Serra-Garcia, V. Peri, R. Süsstrunk, O. R. Bilal, T. Larsen, L. G. Villanueva, and S. D. Huber, *Nature (London)* **555**, 342 (2018).
- [21] X. Ni, M. Weiner, A. Alù, and A. B. Khanikaev, *Nat. Mater.* **18**, 113 (2019).
- [22] H. Xue, Y. Yang, F. Gao, Y. Chong, and B. Zhang, *Nat. Mater.* **18**, 108 (2019).
- [23] S. Imhof, C. Berger, F. Bayer, J. Brehm, L. W. Molenkamp, T. Kiessling, F. Schindler, C. H. Lee, M. Greiter, T. Neupert, and R. Thomale, *Nat. Phys.* **14**, 925 (2018).
- [24] F. J. Wegner, *J. Math. Phys.* **12**, 2259 (1971).
- [25] M. E. Peskin, *Ann. Phys.* **113**, 122 (1978).
- [26] C. Dasgupta and B. I. Halperin, *Phys. Rev. Lett.* **47**, 1556 (1981).
- [27] N. Read and S. Sachdev, *Phys. Rev. Lett.* **62**, 1694 (1989).
- [28] N. Read and S. Sachdev, *Nucl. Phys. B* **316**, 609 (1989).
- [29] E. Fradkin and S. Kivelson, *Mod. Phys. Lett. B* **04**, 225 (1990).
- [30] M. Hermele, M. P. A. Fisher, and L. Balents, *Phys. Rev. B* **69**, 064404 (2004).
- [31] R. Moessner, S. L. Sondhi, and E. Fradkin, *Phys. Rev. B* **65**, 024504 (2001).
- [32] G. Baskaran and P. W. Anderson, *Phys. Rev. B* **37**, 580 (1988).
- [33] I. Affleck and J. B. Marston, *Phys. Rev. B* **37**, 3774 (1988).
- [34] P. A. Lee, N. Nagaosa, and X.-G. Wen, *Rev. Mod. Phys.* **78**, 17 (2006).
- [35] J. B. Kogut, *Rev. Mod. Phys.* **51**, 659 (1979).
- [36] J. Dalibard, F. Gerbier, G. Juzeliūnas, and P. Öhberg, *Rev. Mod. Phys.* **83**, 1523 (2011).
- [37] L. Barbiero, C. Schweizer, M. Aidelsburger, E. Demler, N. Goldman, and F. Grusdt, *Sci. Adv.* **5**, eaav7444 (2019).
- [38] M. Aidelsburger, L. Barbiero, A. Bermudez, T. Chanda, A. Dauphin, D. González-Cuadra, P. R. Grzybowski, S. Hands, F. Jendrzejewski, J. Jünemann, G. Juzeliūnas, V. Kasper, A. Piga, S.-J. Ran, M. Rizzi, G. Sierra, L. Tagliacozzo, E. Tirrito, T. V. Zache, J. Zakrzewski *et al.*, *Philos. Trans. R. Soc. A* **380**, 20210064 (2022).
- [39] R. Nandkishore, M. A. Metlitski, and T. Senthil, *Phys. Rev. B* **86**, 045128 (2012).
- [40] S. Gazit, M. Randeria, and A. Vishwanath, *Nat. Phys.* **13**, 484 (2017).
- [41] E. H. Lieb, *Phys. Rev. Lett.* **73**, 2158 (1994).
- [42] S. Gazit, F. F. Assaad, S. Sachdev, A. Vishwanath, and C. Wang, *Proc. Natl. Acad. Sci.* **115**, E6987 (2018).
- [43] F. F. Assaad and T. Grover, *Phys. Rev. X* **6**, 041049 (2016).
- [44] C. Prosko, S.-P. Lee, and J. Maciejko, *Phys. Rev. B* **96**, 205104 (2017).
- [45] E. J. König, P. Coleman, and A. M. Tsvelik, *Phys. Rev. B* **102**, 155143 (2020).
- [46] U. Borla, B. Jeevanesan, F. Pollmann, and S. Moroz, *Phys. Rev. B* **105**, 075132 (2022).
- [47] Y. Prasad, A. Medhi, and V. B. Shenoy, *Phys. Rev. A* **89**, 043605 (2014).
- [48] A. Haldar and V. B. Shenoy, *Sci. Rep.* **4**, 6655 (2014).
- [49] I. S. Tupitsyn, A. Kitaev, N. V. Prokof'ev, and P. C. E. Stamp, *Phys. Rev. B* **82**, 085114 (2010).
- [50] In a system with periodic boundary conditions, there will be four distinct sets of $z_{Ja,\alpha}$ for a given set of B_p . These correspond to different values of the global Wilson line operators. On a finite system with periodic boundary conditions, one of the configurations will be chosen for the ground state in the presence of fermions. The one chosen will typically correspond with that configuring $z_{Ja,\alpha}$ whose Wilson line eigenvalues will be unity, and the fermions do not experience any flux enclosed along either direction of the torus.
- [51] See Supplemental Material at <http://link.aps.org/supplemental/10.1103/PhysRevB.107.245142> for symmetry invariants of the band insulators, filling anomaly, symmetries of the half-filled Hubbard model, discussion of the Gross-Neveu model, renormalization group analysis of the Gross-Neveu model, and Schwinger boson mean-field theory.
- [52] W. A. Benalcazar, T. Li, and T. L. Hughes, *Phys. Rev. B* **99**, 245151 (2019).
- [53] F. Schindler, M. Brzezińska, W. A. Benalcazar, M. Iraola, A. Bouhon, S. S. Tsirkin, M. G. Vergniory, and T. Neupert, *Phys. Rev. Res.* **1**, 033074 (2019).
- [54] A. Kitaev, *Ann. Phys.* **303**, 2 (2003).
- [55] D. P. Arovas, E. Berg, S. A. Kivelson, and S. Raghu, *Annu. Rev. Condens. Matter Phys.* **13**, 239 (2022).
- [56] C. N. Yang and S. Zhang, *Mod. Phys. Lett. B* **04**, 759 (1990).
- [57] A. Abanov and P. Wiegmann, *Nucl. Phys. B* **570**, 685 (2000).
- [58] H. Kleinert and V.-S. Frohlinde, *Critical Properties of ϕ^4 Theories* (World Scientific Publishing Company, 2001).
- [59] J. Gracey, *Nucl. Phys. B* **341**, 403 (1990).
- [60] P. Ghaemi and S. Ryu, *Phys. Rev. B* **85**, 075111 (2012).
- [61] R. Boyack, H. Yezhakov, and J. Maciejko, *Eur. Phys. J.: Spec. Top.* **230**, 979 (2021).
- [62] M. Matsumoto, C. Yasuda, S. Todo, and H. Takayama, *Phys. Rev. B* **65**, 014407 (2001).
- [63] A. Auerbach and D. P. Arovas, *Phys. Rev. Lett.* **61**, 617 (1988).
- [64] S. Sarker, C. Jayaprakash, H. R. Krishnamurthy, and M. Ma, *Phys. Rev. B* **40**, 5028 (1989).
- [65] A. Auerbach, *Interacting Electrons and Quantum Magnetism* (Springer, New York, 1998).
- [66] S. Furukawa, T. Dodds, and Y. B. Kim, *Phys. Rev. B* **84**, 054432 (2011).
- [67] A. Rüegg, S. D. Huber, and M. Sigrist, *Phys. Rev. B* **81**, 155118 (2010).